

# Inhibition of False LandMarks

Debora Gil and Petia Radeva

Centre de Visió per Computador - dept. Informàtica, UAB  
*Edifici O - Campus UAB, 08193 Bellaterra, Barcelona, Catalonia, Spain*  
*debora, petia @uab.es*

**Abstract.** We argue that a corner detector should be based on the degree of continuity of the tangent vector to the image level sets, work on the image domain and need no assumptions on neither the image local structure nor the particular geometry of the corner/junction. An operator measuring the degree of differentiability of the projection matrix on the image gradient fulfills the above requirements. Its high sensitivity to changes in vector directions makes it suitable for landmark location in real images prone to need smoothing to reduce the impact of noise. Because using smoothing kernels leads to corner misplacement, we suggest an alternative fake response remover based on the receptive field inhibition of spurious details. The combination of both orientation discontinuity detection and noise inhibition produce our Inhibition Orientation Energy (IOE) landmark locator.

## 1 Introduction

The ability of our receptive system to detect sudden changes in the surrounding environment has been often used in computer vision to extract the key image features. However the visual system perception inhibition principle has been scarcely used in spite of being an efficient noise remover. We suggest using inhibition of image discontinuities to design a landmark detector based on corner/junction location. Current corner detectors (see [11] for an exhaustive review) split into those working on the image (2D) domain and those ones that analyze the (1D) geometry of some curves extracted from the image.

Most 2D operators, either explicitly or implicitly, search for corners with a particular angulation, which makes them unable to detect junctions and mares their performance in real images. Response of operators measuring image isotropy ([3], [7]) drops at acute angles and their performance substantially worsens with noise or textured backgrounds. Parametric approaches [10], [12] fit an analytic model of a corner to the particular image they handle. Besides being time consuming, they are prone to poorly perform in real images as they assume uniform grey level within regions. Wedge filters need no assumptions on image intensity but, by their own design, they only respond to a given set of corner angulation and orientations [9], [13]. Only curvature-based algorithms and the simple SUSAN [14] comparison of grey values need no assumptions on the corner geometry. The degree of differentiability in the image required to compute curvature is not satisfied at corners, which may lead to ambiguous results. Although the SUSAN scheme works fine without any requirements on the image differentiability or local structure, it sometimes confuses edges and corners on real images.

On the other side, algorithms running on curves extracted from the image mainly search for discontinuities on the curve tangent vector. Wavelets [5], [8], [16] are a usual tool to analyze such regularity because of their robust high response near points of discontinuity [6].

Although we agree in the former definition of corner, working on image contours instead that on the image domain has several disadvantages. First, the compulsory previous extraction of image edges, which need to be closed contours, leads to some sort of boundary tracking [5], [15] to fill-in edge gaps at corners. Second, computation of tangent spaces of curves in parametric form is a delicate step [5], [16] that would be unnecessary in their implicit level set original form.

In any case, all algorithms must reject the operator response to texture and noise by working on a smoothed version of the original image. This smoothing can be achieved by either straight convolution of the image with a gaussian kernel or, in the case of wavelets and scale-space approaches, working at coarse scales/level of detail. A major drawback of both strategies is that image prominent features are blurred in the measure noise is reduced. Although there are some criteria [8] to determine the proper resolution, corner misplacement is difficult to avoid unless some sort of corner tracking [5], [15] through all levels of detail is performed.

In this paper we characterize corners and junctions in terms of the lack of continuity of the projection matrix onto the image unit gradient. Convolution with first derivatives of oriented anisotropic gaussian kernels are used to determine the matrix singular points. We will refer to this orientation continuity energy as Orientation Energy, OE for short. Because it does not rely on either the local image structure or a particular model of corner/junction, our operator characterizes both corners and junctions without any possible confusion with other image salient features. Besides OE increases as the corner angle becomes more acute, in contrast to operators measuring isotropy of the image ([3], [7]), which response drops for angles less than 90 degrees. Finally, by scanning the image in all possible orientations in the discrete domain, our operator is capable of detecting corners without any sort of fitting ([10], [12]) or special filter design ([9], [13]).

Still fake responses at noisy or textured backgrounds must be suppressed. Instead of running our operator at different scales [15],[5], we propose using the same mechanisms that serve our visual system to ignore noise and texture. Our sensitivity to abrupt changes differs depending on the nature of the response in the surroundings: only isolated or unique salient features are taken into account. In [1] this biological mechanism has been modelled by means of an inhibition kernel, which convolved with the image Gabor energy resulted in a robust edge detector. In our case, we will apply inhibition to a representation of the image salient features obtained by means of the energy of the image wavelet transform. This map of the most significant image features is the input for OE and its inhibition serves as a noise suppression factor for IOE. Because the former strategy does not hinge upon any smoothing or level of detail, our operator can work at the finest scale, thus ensuring maximum location accuracy. Experiments on synthetic noisy images prove IOE better performance and landmark extraction in real images shows its higher applicability and reliability.

We have structured the paper as follows. Section 2 is devoted to the description of IOE, validation on synthetic corners and landmark location in real images are presented in Section 3 and conclusions are exposed in Section 4.

## 2 From Wavelets to Corners

A usual way of describing corners is as points of maximal curvature of the image level sets. Not only is this definition ambiguous but also incorrect. Ambiguity comes from the fact that, in the case of corners of image level sets, image valleys and ridges are also characterized

by maxima of curvature. Imprecision follows because, in fact, corners are points where the level curve fails to be  $\mathcal{C}^1$ , which may hinder performance of any differential operator. A curve fails to be  $\mathcal{C}^1$  at points where its tangent space is not properly defined, that is, points of discontinuity of the curve unit tangent direction. Because the image gradient is perpendicular to its level sets, we conclude that corners and junctions are characterized as discontinuity points of the image unit gradient direction. If  $\nabla u/|\nabla u|$  is the image unit gradient, then the projection matrix,  $P$ , onto the vector space it generates:

$$P = P \left( \frac{\nabla u}{|\nabla u|} \right) = \frac{1}{|\nabla u|^2} \begin{pmatrix} u_x^2 & u_x u_y \\ u_x u_y & u_y^2 \end{pmatrix}$$

has equal degree of differentiability than the vector direction. Therefore, we will consider that a point is a corner/junction if and only if the projection matrix onto the image unit gradient,  $P$ , fails to be continuous. For a robust estimation of the curve normal spaces, the projection matrix will be computed over the eigenvector of maximum eigenvalue of the Structure Tensor [2].

Now, one of the best tools to detect discontinuities and lack of differentiability are wavelets, both from a theoretic [6] and practical point of view [8], [16]. Because we are looking for discontinuities of  $P$  and our domain is two dimensional, we will use first derivatives of oriented anisotropic Gaussian kernels, namely  $G$ . Let  $\sigma = (\sigma_1, \sigma_2)$ , with  $\sigma_1 < \sigma_2$ , be the variance and  $\tilde{x}, \tilde{y}$  the coordinates given by the rotation:

$$\begin{pmatrix} \tilde{x} \\ \tilde{y} \end{pmatrix} = \begin{pmatrix} \cos(\theta) & \sin(\theta) \\ -\sin(\theta) & \cos(\theta) \end{pmatrix} \begin{pmatrix} x \\ y \end{pmatrix}$$

Given the first derivative of  $G$  along its minor axis  $\tilde{x}$ : with  $G$  first derivative along its minor axis  $\tilde{x}$ :

$$MH_\theta = \partial_{\tilde{x}}(G) = \partial_{\tilde{x}} \left( \frac{1}{2\pi\sigma_1\sigma_2} e^{-\frac{\tilde{x}^2}{2\sigma_1^2} - \frac{\tilde{y}^2}{2\sigma_2^2}} \right) = -\tilde{x}G/\sigma_1^2$$

Its convolution with an image  $u(x, y)$  yields the oriented wavelet coefficient:

$$W_\theta u(x, y) = \int MH_\theta(\tilde{x} - x, \tilde{y} - y)u(\tilde{x}, \tilde{y})d\tilde{x}d\tilde{y}$$

The  $L^2$  norm of the above coefficients with respect to the angular parameter is an energy,  $E$ , that measures the image degree of continuity at a given scale/level of detail. In the case of a matrix  $P$ , its wavelet transform is another matrix. Therefore  $E$  must be the integral (over all orientations) of the norm of  $P$  as linear transformation. In our particular case the  $L^2$  norm of the transformed matrix is given by its determinant. The Orientation Energy we suggest is:

$$OE(x, y) = OE_u = \int (detW_\theta P_u)^2 d\theta \quad (1)$$

Corners correspond to local maxima. Response at textured backgrounds need to be suppressed in real images landmark location. To avoid such false corners we propose using an inhibition kernel as in [1]. The main idea is to emulate the human vision system that inhibits its response at discontinuities located in areas presenting a similar singularity at all points. To such purpose, we will work with a representation of the image salient features.

## 2.1 The inhibition of false landmarks

Because wavelets model human vision response, we will use a family of wavelets responding to edges and ridges to obtain a representation of the image salient features [6]. First and second derivatives of anisotropic gaussian kernels in the direction of their minor axis will be our set of wavelets. If  $W_\theta^1, W_\theta^2$  denote the wavelet coefficients, then the energy:

$$MHE(x, y) = \int (W_\theta^1 u)^2 + (W_\theta^2 u)^2 d\theta$$

yields an image close to the representation that human perception yields. The inhibition factor is computed by convolving MHE with a ring-shaped inhibition kernel:

$$IK = \frac{1}{\|H(DG_\sigma)\|_2} H(DG_\sigma), \quad H(z) = \begin{cases} 0 & z < 0 \\ z & z \geq 0 \end{cases}$$

where  $\|\cdot\|_2$  denotes the  $L^2$  norm and  $DG_\sigma$  is the following difference of gaussian functions:

$$DG_\sigma = \frac{1}{2\pi(4\sigma)^2} e^{-\frac{x^2+y^2}{2(4\sigma)^2}} - \frac{1}{2\pi\sigma^2} e^{-\frac{x^2+y^2}{2\sigma^2}}$$

The positive response of the difference:

$$IA = H(MHE - IK * MHE)$$

is added as a noise remover factor to the energy (1) computed on MHE.

## 3 Experiments

We present two different experiments: assessment of performance and landmark extraction in real images. In all experiments, we use a scale  $\rho = 0.5$  for the structure tensor and 6 orientations with  $\sigma = 1$  for the wavelet kernels used in OE and MHE. The threshold used for corner extraction corresponds to the 99.5% percentil of IOE values.

### 3.1 Synthetic Corners

We have compared IOE to the curvature-based (CURV) corner detector of [4], Harris [3] and SUSAN [14]. We have applied them to a set of 9 corners with angles in the range  $[20, 180^\circ]$  in images corrupted with gaussian noise of  $\sigma = 0, 0.1, 0.25, 0.5$ . As in [11], performance is measured in terms of location accuracy and trade-off between true and false detections. We consider a positive response is correct if it lies in a  $7 \times 7$  window centered at the true corner, including the flat case (180). Plots in fig2 show the total number (for all noises) of true/false detections for each angle (abscissa axis). Images in fig.3.1 show the detections (squares on noise free angles) for an acute corner, an angle near  $90^\circ$  and the flat case, for  $\sigma = 0.25$  (images in 1st column).

Statistics for the ideal detector should yield 0 false detections, 4 good responses (1 for each noisy case) for angles less than  $\pi$  and no response for flat angles. Due to sensitivity to lack of differentiability, curvature-based algorithms fail to detect the most acute angles (1st image in 2nd column of fig.3.1) and produce false responses as noise increases. Harris

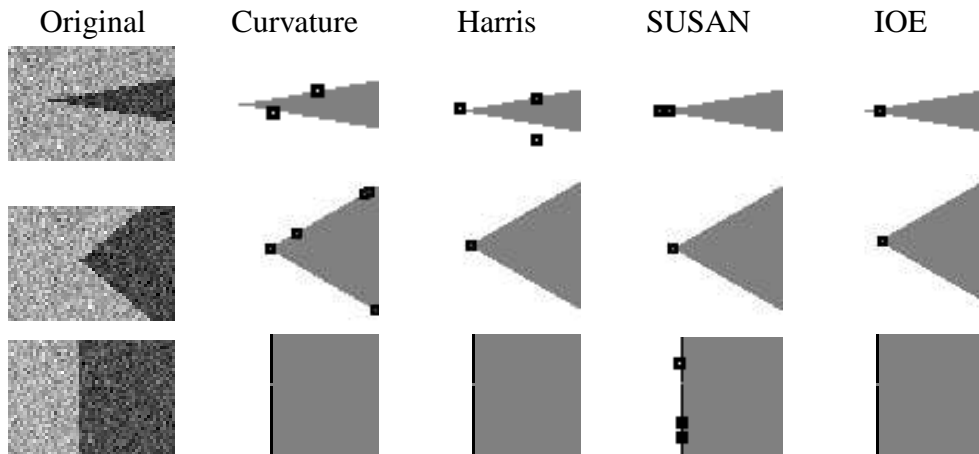


Figure 1: Synthetic Noisy Corners: 1st row acute angle, 2nd right and 3rd flat

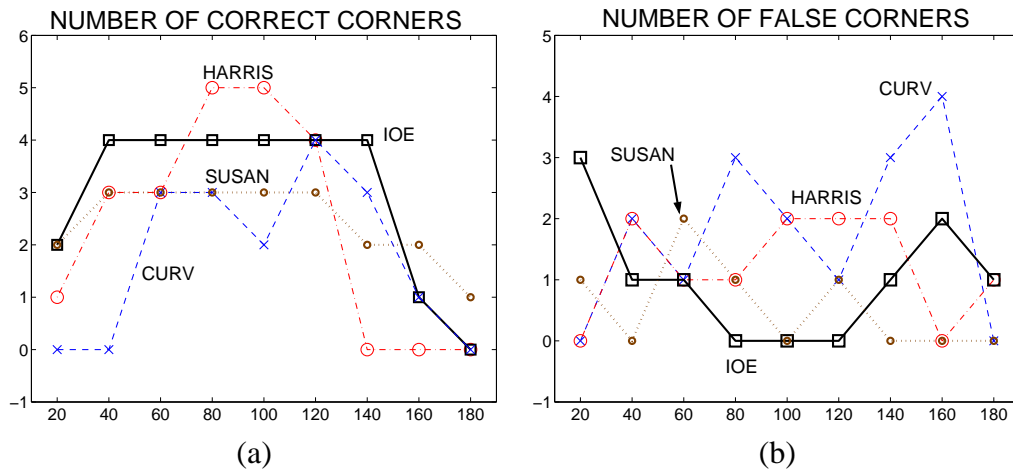


Figure 2: Statistics for Synthetic Corners

number of detections drops as image anisotropy increases, which difficulties detection of acute corners (1st image in 3rd column of fig.3.1) and increases the number of false positives in the presence of noise (it is the worst performer with up to 4 wrong responses). SUSAN numbers would match the ideal case, if it were not for its response at flat angles (last image in 4th column of fig.3.1) and random false detections due to noise(see plot of fake detections in fig.2(b)). Finally, 4 right detections with 1 false one at most for angles between  $[40, 140]$  and null response at 180, select IOE as the algorithm that best matches the ideal figures.

### 3.2 Landmark extraction in real images

Choosing the best performers of Experiment 3.1, we have applied IOE and SUSAN to landmark location on real images. The set of test images include geometric patterns (building in background of boat image in fig.3(a) and strips in shirt of fig.4(a)), faces (portrait in fig.4(a)) and natural scenes with texture (fig.6(a), (b)).

In general terms the number of false landmarks at edges and texture backgrounds is larger for the SUSAN scheme. Points on the border of the wooden platform and at the foreground building in fig.3(c) correspond to edges rather than to landmarks. In a similar fashion, SU-

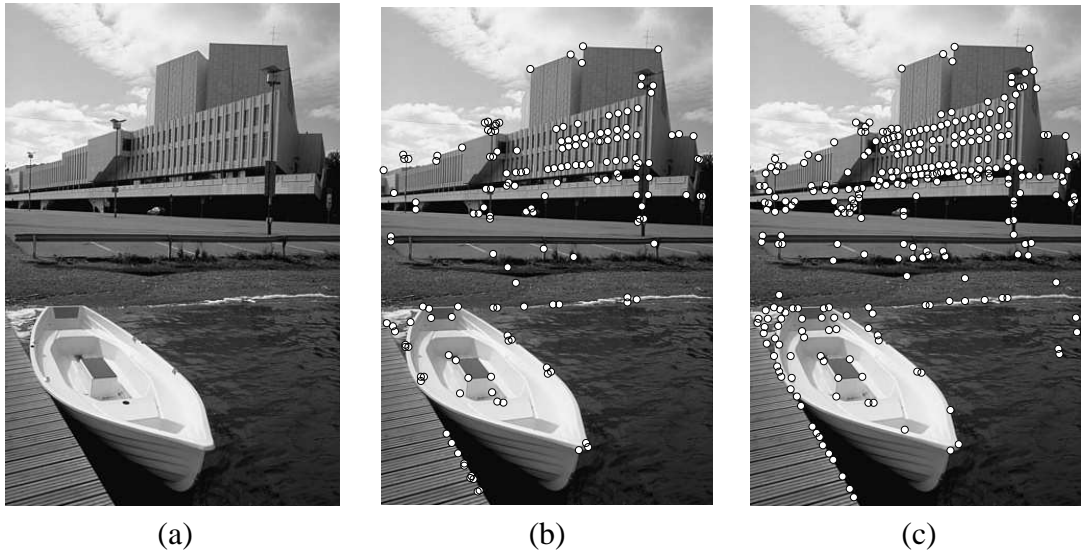


Figure 3: Landmarks in Real Images I: Original (a), IOE (b) and SUSAN (c)

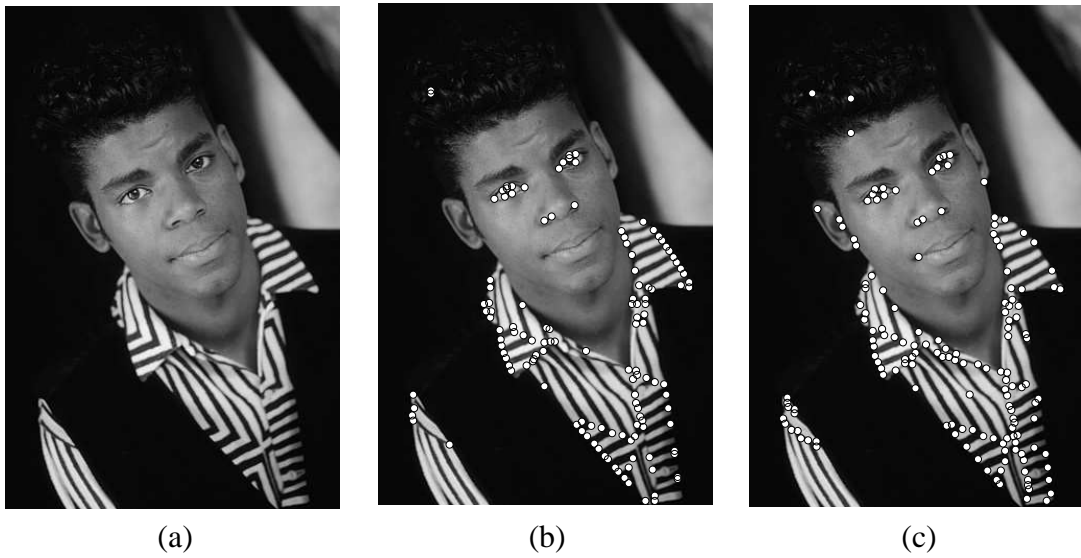


Figure 4: Landmarks in Real Images II: Original (a), IOE (b) and SUSAN (c)

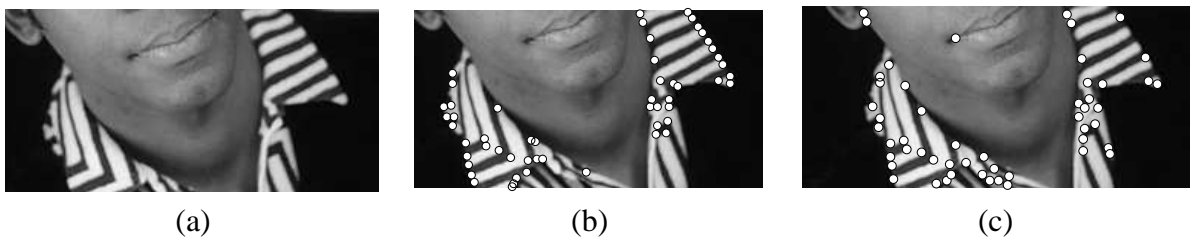


Figure 5: Landmarks closed-up: Original (a), IOE (b) and SUSAN (c)

SAN yields an over response at shirt stripes (like the line on the man shoulder in fig.4(c)) and branches silhouette (fig.6(c)), with the majority of points detected as landmarks. Textures produce some erratic false positives in water waves (right side of fig.3(c)), boys' hair (fig.4(c)) and interior of branches (fig.6(e)). In the case of the strong patterned nest in (fig.6(f)) the

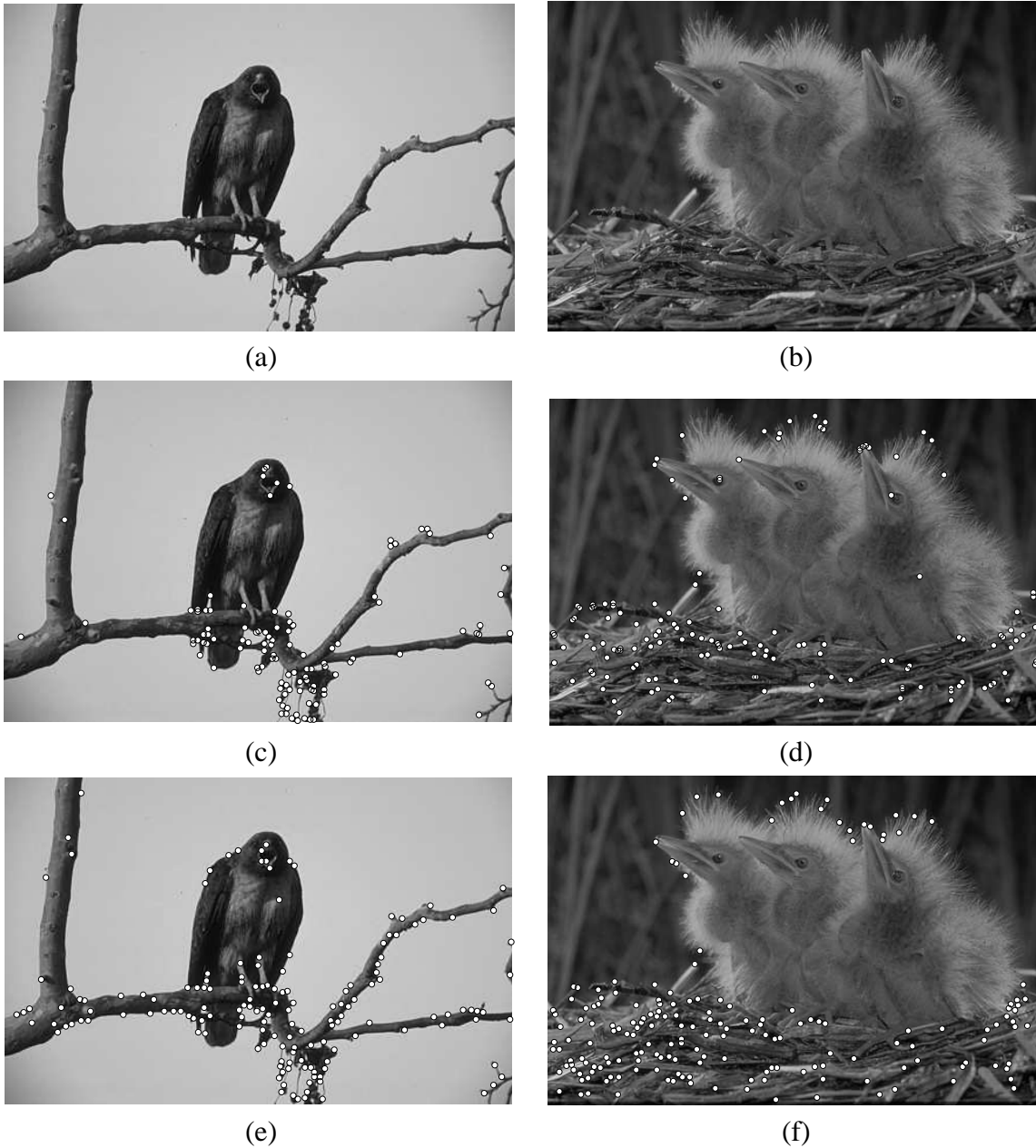


Figure 6: Landmarks in Natural Scenes: Original (a), (b), IOE (c),(d) and SUSAN (e), (f)

number of fake detections includes almost all points. Still, despite this sensitivity to corners not all stripe corners (see closed up in fig.5(c)) and birds beaks have been properly located by SUSAN.

On the other hand, IOE detects most geometric corners yielding optimal responses at windows and boat corners (fig.3(b)) and shirt stripes (fig.4(b)). Close-ups of the man shirt in fig.5 show IOE higher accuracy (fig.5 (b)) compared to SUSAN (fig.5 (c)). On the other hand, IOE performance for natural scene corners and T-junctions is also competitive: branches junctions and birds' beaks (fig.6(c), (d)) have been perfectly extracted. The impact of the inhibition term is determinant for IOE to yield a minimum number of fake landmarks. It lacks of response at the slightly texture induced by water waves and curly hairs and at the birds nest it gives a substantially less number of fake positives than SUSAN.

## 4 Conclusions

In the present paper, we define an operator that measures the continuity of the image unit gradient direction. The norm of the wavelet transform of the projection matrix onto the latter is an energy that increases with corner acuteness. In order to ensure maximum location accuracy, we propose a scale independent noise response suppressor. Basing on the ability of the visual receptive cells to inhibit their response at homogeneous noisy areas, fake responses are removed by means of the convolution of the image wavelet energy with an inhibition kernel.

Our combination of inhibition of uniform discontinuities yields a corner detector reliable enough as to robustly extract landmarks in real images. Statistics on synthetic corners and results on natural scenes prove the higher efficiency of our operator compared to usual techniques. Results on natural scenes with textured backgrounds prone to produce false responses show its applicability.

## References

- [1] C.Grigorescu, N.Petkov, M.A. Westenberg. *Contour Perception Based on Non-Classical Receptive Field Inhibition*, IEEE Trans. Imag. Proc., vol 12, no. 7, 2003.
- [2] B.Jahne. *Spatio-temporal Image Processing: Theory and Scientific Applications*, Springer-Verlag Berlin 1993.
- [3] C.Harris, M.Stephens. *A combined Corner and Edge Detector*, Proc. 4th Alvey Vision Conf., 1988.
- [4] L.Kitchen, A.Rosendfeld. *Gray-level corner Detection*, Patt. Recog. Letters, vol. 1 (95-102), 1982.
- [5] J.S.Lee, Y.N.Sun, C.H.Chen. *Multiscale Corner Detection by Wavelet Transform*, IEEE Trans. Imag. Proc., vol.4, 1995.
- [6] S.Mallat. *A wavelet tour of Signal Processing*, Academic Press, INC, 1999.
- [7] J.A. Noble. *Finding Corners*, Imag. Vis. Comp. 6:2, 1988.
- [8] A.Qudus, M.Gabbouj. *Wavelet-based corner detection technique using optimal scale*, Patt. Recog. Letters, 23, 2002.
- [9] B.Robbins, R.Owens. *2D Feature Detection via Local Energy*, Imag. Vis. Comp. 15, 1997.
- [10] K.Rohr. *Recognizing Corners by Fitting Parametric Models*, Int. J. Comp. Vision, 9:3, 1992.
- [11] K.Rohr. *LandMark-based Image Analysis. Using geometric and intensity models*, Kluwer Academic Publishers, 2001.
- [12] P.L.Rosin. *Measuring Corners Properties*, Comp. Vis. Imag. Unders., vol. 73, n2, 1999.
- [13] E.P.Simoncelli, H.Farid. *Steerable Wedge Filters for Local Orientation Analysis*, IEEE Trans. Imag. Proc., vol.5 (9), 1996.
- [14] S.M.Smith, J.M.Brady. *SUSAN-A New Approach to Low Level Image Processing*, Int. J. Comp. Vision, 23:1, 1997.
- [15] F.Mokhtarian, R.Suomela. *Robust Image Corner Detection through Curvature Scale Space*, TPAMI, vol. 12 (12), 1998.
- [16] C.Yeh, *Wavelet-based detection using eigenvectors of covariance matrices*, Patt. Recog. Letters, 24, 2003.